AD-A094 415   SRI INTERNATIONAL MENLO PARK CA   F/G 20/11
HIGH TEMPERATURE OXIDATION AND MECHANICAL PROPERTIES OF SILICON--ETC(U)
NOV 80 D CUBICCIOTTI, K H LAU, D J ROWCLIFFE   F44620-76-C-0116
UNCLASSIFIED   SRI-5522-4   AFOSR-TR-81-0031   NL

1 OF 1
AD
A094415

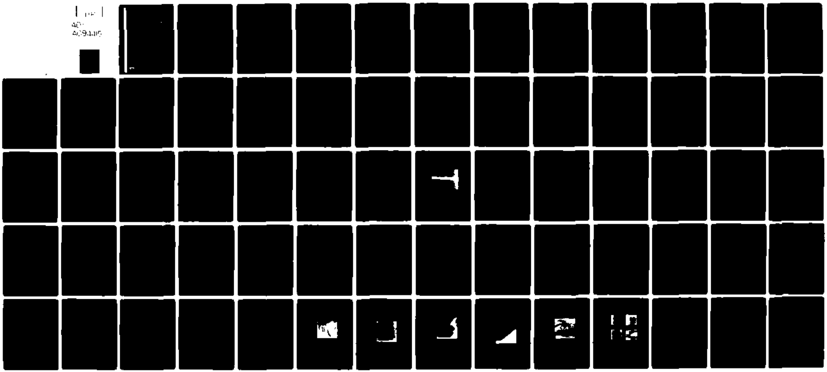

END
DATE
FILMED
2-81
DTIC

AFOSR-TR- 81-0031

(12)

AD A094415

HIGH TEMPERATURE OXIDATION AND MECHANICAL PROPERTIES OF SILICON NITRIDE

LEVEL II

Final Scientific Report 5522-4
Covering the Period October 1, 1976
through October 30, 1980

DTIC
ELECTE
FEB 0 2 1981
E

November 30, 1980

By: D. D. Cubicciotti, K. H. Lau,
D. J. Rowcliffe, and R. H. Lamoreaux

Prepared for:

Air Force Office of Scientific Research/NE
Building 410
Bolling Air Force Base, D.C. 20332

Attention: Captain S. Wax, Program Manager
Electronic and Solid State Sciences

AFOSR Contract No. F44620-76-C-0116

SRI Project PYU 5522

SRI International
333 Ravenswood Avenue
Menlo Park, California 94025
(415) 326-6200
Cable: SRI INTL MPK
TWX: 910-373-1246

81 2 2 066

UNCLASSIFIED

SECURITY CLASSIFICATION OF THIS PAGE (*When Data Entered*)

(19) REPORT DOCUMENTATION PAGE

READ INSTRUCTIONS
BEFORE COMPLETING FORM

1. REPORT NUMBER (18) **AFOSR TR-81-0031**	2. GOVT ACCESSION NO. AD-A094 415	3. RECIPIENT'S CATALOG NUMBER
4. TITLE (*and Subtitle*) (6) HIGH TEMPERATURE OXIDATION AND MECHANICAL PROPERTIES OF SILICON NITRIDE.		5. TYPE OF REPORT & PERIOD COVERED Final
(14) SRI		6. PERFORMING ORG. REPORT NUMBER -5522-4
7. AUTHOR(s) (10) D. Cubicciotti, K. H. Lau, D. J. Rowcliffe and R. H. Lamoreaux		8. CONTRACT OR GRANT NUMBER(s) NEW (15) F44620-76-C-0116
9. PERFORMING ORGANIZATION NAME AND ADDRESS SRI International Menlo Park, California 94025		10. PROGRAM ELEMENT, PROJECT, TASK AREA & WORK UNIT NUMBERS 61102F (16) 2306 A2 (17)
11. CONTROLLING OFFICE NAME AND ADDRESS Air Force Office of Scientific Research/NE Bolling Air Force Base, D.C. 20332		12. REPORT DATE NOVEMBER 30, 1980
		13. NUMBER OF PAGES 62
14. MONITORING AGENCY NAME & ADDRESS (*if different from Controlling Office*) (11) 30 Nov 80 (12) 6		15. SECURITY CLASS. (*of this report*) UNCLASSIFIED
		15a. DECLASSIFICATION/DOWNGRADING SCHEDULE

16. DISTRIBUTION STATEMENT (*of this Report*)

Approved for public release, distribution unlimited

(9) Final rept. 1 Oct 76 – 30 Oct 80

17. DISTRIBUTION STATEMENT (*of the abstract entered in Block 20, if different from Report*)

18. SUPPLEMENTARY NOTES

19. KEY WORDS (*Continue on reverse side if necessary and identify by block number*)

silicon nitride
ceramics
corrosion
strength
oxidation

20. ABSTRACT (*Continue on reverse side if necessary and identify by block number*)

A summary is presented of the progress made during the four years of an investigation into the high-temperature oxidation and mechanical properties of hot-pressed silicon nitride. Progress during the fourth year of the program is emphasized.

Oxidation rates of magnesia hot-pressed Si_3N_4 were measured for as long as 400 hours in air and 144 hours in SO_2/O_2 at 1643 K. The decrease in oxidation rates observed previously for long exposure times was confirmed to 400 hours.

DD FORM 1 JAN 73 1473 EDITION OF 1 NOV 65 IS OBSOLETE 410281 UNCLASSIFIED

Electron microprobe analyses of samples oxidized 144 hours in air and SiO_2/O_2 at 1643 K revealed a depletion of magnesia in the ceramic. The effect of surface contaminants on oxidation was examined to investigate the cause of strength controlling oxidation pits. The effect of strain on oxidation rate was investigated. Preoxidation followed by surface finishing produced ceramic more resistant to oxidation. The use of controlled oxidation after hot-pressing to adjust the magnesia composition is suggested.

The results of thermogravimentric studies on the rate of oxidation of chemically vapor-deposited Si_3N_4 at various temperatures are reported. Up to about 1725 K, diffusion of oxygen through the oxide scale is the rate-determining oxidation process.

CONTENTS

APPENDICES

BACKGROUND AND TECHNICAL PROGRESS

Silicon nitride (Si_3N_4) has been widely advocated for many high-temperature structural engineering applications.[1-4] One important application is for gas turbines, which are used in propulsion systems for advanced aircraft and for some short-life missiles. The demands for maximum performance and efficiency in such engines necessitate extremely high gas-inlet temperatures that can be withstood only be such ceramics as Si_3N_4. In addition to the potential for increased engine efficiency through higher gas-inlet temperatures, the use of Si_3N_4 to replace currently used Ni-or Co-based superalloys offers a significant weight reduction that can increase the performance of the propulsion system.

Engine demonstration programs are currently being conducted to evaluate the performance of Si_3N_4 components in short-life high-temperature gas turbines. However, a more detailed fundamental understanding of the property changes that occur during use is required before these ceramics qualify for long-term load-bearing applications. Hot corrosion has always been a major cause of failure of conventional turbine components and is expected to be an equally severe problem in a high-temperature ceramic engine. In the case of Si_3N_4, it is generally known that oxidation reduces mechanical performance,[5,6] but the extent of property degradation and the underlying causes have not been well established. Therefore, it is essential to evaluate fully the oxidation behavior of Si_3N_4 and the potentially life-reducing effects of exposure to different oxidizing environments.

TECHNICAL PROGRESS

In response to these needs, SRI International has been studying oxidation and its subsequent effect on the mechanical properties of hot-pressed Si_3N_4. This report describes work performed during the fourth year of the program. Progress during the first three years has been described in our interim reports[7-9] and in journal articles and conference presentations.[10-12] During this time, fundamental studies were made of the oxidation kinetics of two grades of hot-pressed Si_3N_4, Norton NC132, which contains MgO, and Norton NCX34, which contains Y_2O_3. The study of NC132 resulted in the development of an entirely new model of the oxidation of Si_3N_4 containing MgO.[10,11] A similar model was proposed[12] for the oxidation of NCS34 at comparable temperatures, with modifications to allow for the effects of pores in the scale that are formed at high temperatures. To complement these studies, measurements were made of the strength of NC132 following high-temperature oxidation. Examination of specimens with different initial surface finishes showed that subsequent changes in strength were not related in a simple way to the depth of the oxide scale, but were primarily a function of the population of surface defects.

During the third year of the program, we studied the oxidation of chemically vapor-deposited (CVD) Si_3N_4 and set up a system to investigate the oxidation of Si_3N_4 exposed to controlled gas mixtures representative of the combustion products of fuel oils. In work on the effects of oxidation on mechanical properties, we found that the fracture toughness of NC132 changes dramatically in the subscale region developed during long-term oxidation. we showed that corrosion pits formed below the oxide control the strength of NC132 oxidized in air or oxygen. Moreover, these pits contain much more CA and less Mg than the normal scale. These observations are particularly important, since their understanding could provide a means of controlling oxidation-induced degradation of strength in NC132.

During the fourth year our main concern has been to investigate the mechanism of pit formation during high-temperature oxidation of NC132. The following tasks were performed:

(1) Oxidized NC132 samples for up to 400 hours in air and 256 hours in 50 vol% SO_2/50 vol% O_2 at 1370°C.

(2) Examined the effects of preoxidation, prior to surface finishing, on the oxidation resistance and mechanical properties of NC132.

(3) Evaluated the effect of specific surface contaminants in corrosion and pitting on NC132.

(4) Investigated the influence of stress on the rate of oxidation and on the mechanical properties of NC132.

(5) Conducted further microprobe analyses of oxidized and unoxidized NC 132.

This study of oxidation and mechanical properties of NC132 is presented in detail in Appendix A.

During the past year we have also completed a study of the rate and mechanism of oxidation of CVD silicon nitride, using samples provided by United Technologies. The details of this study are given in Appendix B, in the form of an article which has been submitted for publication in the Journal of the Electrochemical Society.

PUBLICATIONS AND PRESENTATIONS

Publications and presentations resulting from the four years of research are listed below.

Publications

1. D. Cubicciotti, K. H. Lau, and R. L. Jones, "The Rate Controlling Process in the Oxidation of Hot-Pressed Silicon Nitride," J. Electrochem. Soc. 124, 1955 (1977).
2. A. G. Evans and R. L. Jones, "An Evaluation of a Fundamental Approach to the Statistical Analysis of Fracture," J. Am. Ceram. Soc. 61, (3-4), 156-160 (1978).
3. D. Cubicciotti and K. H. Lau, "Kinetics of Oxidation of Magnesia Hot-Pressed Silicon Nitride," J. Am. Ceram. Soc. 61, 512 (1978).
4. R. L. Jones and D. J. Rowcliffe, "Tensile Strength Distributions for Silicon Nitride and Silicon Carbide Obtained Using the Expanded Ring Test," Am. Ceram. Soc. Bull. 58, 836 (1979).
5. D. Cubicciotti and K. H. Lau, "Kinetics of Oxidation of Yttria Hot-Pressed Silicon Nitride," J. Electrochem. Soc. 126, 771 (1979).
6. R. L. Jones and D. J. Rowcliffe, "The Use of Notched Beams to Measure the Toughness of Ceramics," J. Am. Ceram. Soc. Bull. 58. 1195 (1979).
7. R. H. Lamoreaux, K. H. Lau, and D. D. Cubicciotti, "Kinetics of Oxidation of Chemically Vapor-Deposited Silicon Nitride," submitted to J. Electrochem. Soc.

Presentations

1. K. H. Lau, "Mechanism of Oxidation of Magnesia Hot-Pressed Silicon Nitride," Fall Meeting of the Basic Science Division of American Ceramic Society, Hyannis, Massachusetts, September 1977.
2. D. Cubicciotti, "Oxidation of Yttria Hot-Pressed Silicon Nitride," Electrochemical Society National Meeting, Symposium on Oxidation of Metals and Alloys, Dedicated to the Memory of Carl Wagner, May 1978.
3. K. H. Lau, "Kinetics of Oxidation of Yttria Hot-Pressed Silicon Nitride," Fall Meeting of American Ceramic Society, November 1978.

4. R. L. Jones and D. J. Rowcliffe, "Oxidation-Induced Strength Degradation and Enhancement in Hot-Pressed Si_3N_4," Fall Meeting of the American Ceramic Society, November 1978.

5. D. Cubicciotti, "Oxidation of Silicon Nitride," California Ceramics Club Meeting, SRI International, Menlo Park, California, January 1979.

6. D. J. Rowcliffe, "Ceramics for High Temperature Structural Applications," Stanford University Seminar, Stanford, California, March 1979.

7. D. J. Rowcliffe, "Application of Ceramics to Advanced Heat Engines," University of Santa Clara Seminar, Santa Clara, California, May 1979.

8. D. Cubicciotti, "The Oxidation of Silicon Nitride," invited presentation to the Gordon Research Conferences on Corrosion, July 1979.

9. D. Cubicciotti, "The Oxidation of Ceramic Materials at High Temperatures," invited presentation to the Gordon Research Conference on Ceramics, August 1979.

10. K. H. Lau and D. J. Rowcliffe, "Oxidation of Sintered Silicon Nitride," Annual Meeting of American Ceramic Society, Cincinnati, Ohio, April 1979.

11. D. J. Rowcliffe, "The Effect of Oxidation on the Mechanical Behavior of Silicon Nitride," California Ceramics Club Meeting, Rockwell International, Thousand Oaks, California September 1979.

12. D. J. Rowcliffe and R. H. Lamoreaux, "Effect of Oxidation on the Mechanical Properties of Commercial Si_3N_4," Pacific Coast Regional Meeting of American Ceramic Society, San Francisco, California, October 1980.

REFERENCES

1. W. L. Wallace, "Ceramic Components for Turbine Engines, Phase I," Technical Report 21-2794(03), AFML/AFAPL Contract F336-15-77-C-5171, Garrett-Airesearch Company (November 1978).

2. A. F. McClean and E. A. Fisher, "Brittle Materials Design, High Temperature Gas Turbine," AMMRC CTR 77-20 (August 1977).

3. R. J. Bratton and D. G. Miller, "Brittle Materials Design, High Temperature Gas Turbine," AMMRC (TR-76-3), Vol. 1 (December 1976).

4. R. E. Wallace et al., "Ceramic Gas Turbine Engine Demonstration Program," Interim Report No. 5, Contract N00024-76-C-5352, Airesearch Report 76-212188(5) (May 1977).

5. D. J. Rowcliffe and P. A. Huber, "Hot Gas Stress Corrosion of Silicon Nitride and Silicon Carbide," Proc. Brit. Ceram. Soc. 25, 239 (1975).

6. D. W. Richerson and T. M. Yonushonis, "Effect of Surface Condition on the Strength of Hot-Pressed Si_3N_4," Paper 90-BEN-76P presented at American Ceramic Society Meeting, San Francisco, California (November 1976).

7. D. Cubicciotti, K. H. Lau, and R. L. Jones, "High Temperature Oxidation and Mechanical Properties of Silicon Nitride," SRI Interim Report 5522-1, Contract F44620-76-0116, SRI International, Menlo Park, California (November 1977).

8. D. Cubicciotti, K. H. Lau, R. L. Jones, and D. J. Rowcliffe, "High Temperature Oxidation and Mechanical Properties of Silicon Nitride." SRI Interim Report 5522-2, Contract F44620-76-C-0116, SRI International, Menlo Park, California

9. D. Cubicciotti, K. H. Lau, D. J. Rowcliffe, and R. Lamoreaux, "High Temperature Oxidation and Mechanical Properties of Silicon Nitride," SRI Interim Report 5522-3, Contract F44620-76-C0116, SRI International, Menlo Park, California (November 1979).

10. D. D. Cubicciotti, R. L. Jones, and K. H. Lau, "The Rate Controlling Process in the Oxidation of Hot-Pressed Silicon Nitride," J. Electro-Chem. Soc. 124, 1955 (1977).

11. D. D. Cubicciotti and K. H. Lau, "Kinetics of Oxidation of Magnesia Hot-Pressed Silicon Nitride," J. Amer. Ceram. Soc. 61, 512 (1978).

12. D. D. Cubicciotti and K. H. Lau, "Kinetics of Oxidation of Yttria Hot-Pressed Silicon Nitride," J. Electrochem. Soc. 126, 1723 (1979).

Appendix A

HIGH-TEMPERATURE OXIDATION AND ENVIRONMENTAL EFFECTS ON THE MECHANICAL PROPERTIES OF NC123 MAGNESIA HOT-PRESSED SILICON NITRIDE

SUMMARY

Measurements of weight gains during oxidation at 1370°C[1-5] have been extended to 400 hours in air and to 256 hours in a 50 vol% SO_2/50 vol% O_2 mixture. Weight gains in SO_2/O_2 were similar to those in air for similar exposures. The strength degradation in SO_2/O_2, less severe than in air for times up to 64 hours, was essentially the same as that in air for longer exposures. The rate of weight gain and strength degradation in air at 1370°C were higher for specimens experiencing a static bending stress.

Electron microprobe analysis of specimens oxidized for 144 hours in air and in SO_2/O_2 showed extensively depletion of Mg and Ca in the body of the ceramic, and no penetration of the ceramic by sulfur.

The effects of surface contaminants on pitting of the ceramic during oxidation were investigated and classified according to the depth of scale formed and size of pits produced during standard oxidation treatments.

Rates of oxidation were studied for samples preoxidized before surface finishing. Lower oxidation rates were found for these samples. Preoxidation as a means of adjusting magnesia composition and lowering the tendency to form pits is discussed.

HIGH TEMPERATURE OXIDATION IN AIR AND IN O_2/SO_2

A. Weight Gain Studies

Specimens of NC132 were exposed at 1370°C for up to 400 hours in air, and for up to 256 hours in a 50 vol% SO_2/50 vol% O_2 mixture. The specimens were rectangular bars cut from material designated Billet 2, obtained from Norton Company. A typical analysis of billets made from the powder lot used for Billet 2 is given in Table 1. The bend-test bars were about 3 x 3 x 50 mm in size, and were surface ground in the direction parallel to the specimen length with a 220-grit diamond wheel. Unless otherwise stated, six bars were used for each test.

Results of the weight gain measurements are shown in Figure 1, a plot of the mean $(\text{weight gain/area})^2$ versus time at 1370°C. The recently published results of Palm and Greskovich[6] for oxidation of NC132 in air at 1405°C are included for comparison. The solid line through the data points was derived by fitting our data points in air to the power law expression,

$$(\text{weight gain/area}) = a\ (\text{time})^b \qquad (1)$$

where it was found that $a = 3.2994\ g/m^2$ and $b = 0.3117$.

Several features are apparent from this graph. Agreement between our results and those of Palm and Greskovich is excellent. The results for oxidation in SO_2/O_2 are scattered about the results for oxidation in air. Oxidation for times greater than about 20 hours slows progressively from the apparent parabolic behavior found for short-term oxidation.[1] The lower oxidation rate for long exposure is consistent with the mechanism of oxidation, in which the oxidation rate is controlled by the diffusion of magnesium from the ceramic into the silicate scale,[4,5] and with the decrease in the bulk magnesium content found in the microprobe

Table 1

TYPICAL ANALYSIS OF NC132 BILLETS MADE FROM HN-10 POWDER

Impurity	Weight Percent*
Al	0.21
Ca	0.01
Fe	0.20
Mg	0.8
O	2.6
W	0.92

*Values are typical data obtained from Norton Company, Worcester, Massachusetts

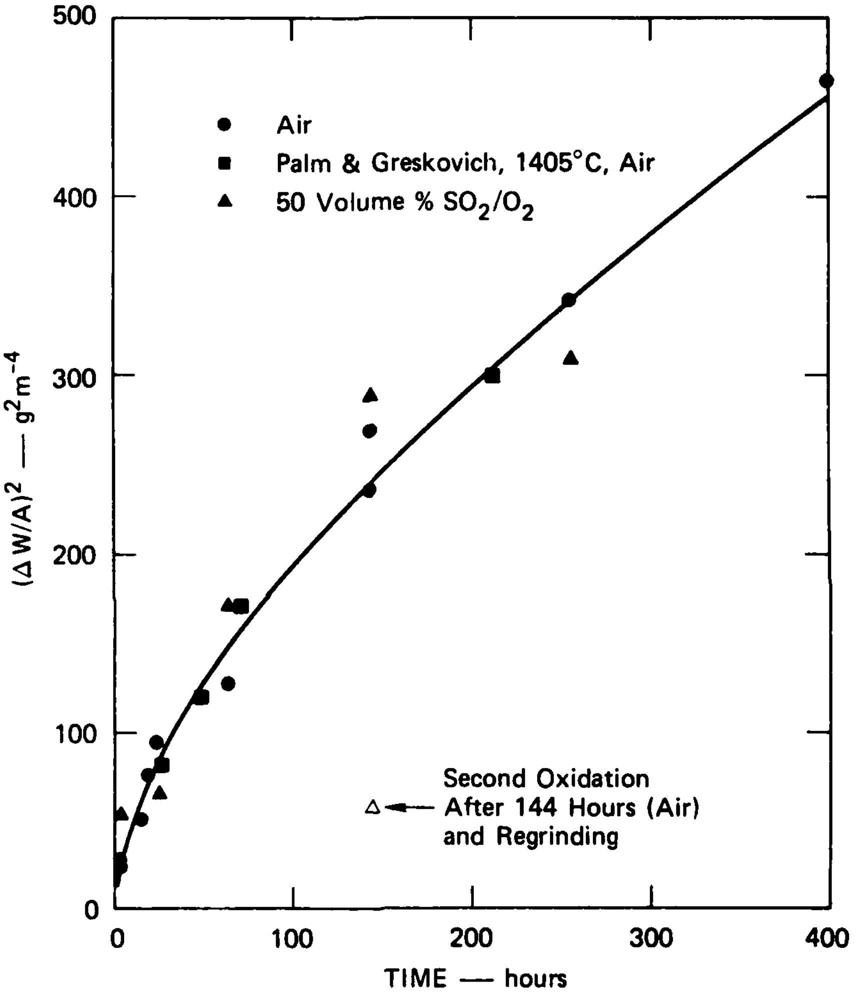

SA-5522-87R

FIGURE 1 PARABOLIC PLOT OF THE OXIDATION OF NC132 HOT-PRESSED Si_3N_4 AT 1643 K IN AIR AND IN 50 vol % SO_2/50 vol % O_2

studies outlined below. In effect, when the magnesium content throughout the sample is lowered from the original value, the diffusion of magnesium is better approximated by a "finite slab" model than the "semi-infinite slab" model which predicts a linear relationship between (weight gain/area)^2 and time.

B. Strength Studies

Effects of oxidation in air and in 50 vol% SO_2/50 vol% O_2 at 1370°C on the strength of NC132 were reported in the third Interim Report[3] for time to 256 hours in air and 64 hours in SO_2/O_2. These studies indicate that strengths of specimens oxidized in air at 1370°C decreased at a rate which lessened with time, to the degree that the strength found after 256 hours was the same as after 144 hours. For exposure to 64 hours, the strength of specimens oxidized in SO_2/O_2 was greater than that of specimens similarly oxidized in air. Oxidation pits formed at the Si_3N_4-oxide scale interface were found to control the strength of the ceramic, and the linear correlation shown in Figure 2 between specimen strengths and the square root of the pit diameters was established. Calcium was found in higher-than-average concentration in the oxidation pits. The lower rate of strength degradation and decreased incidence of oxidation pits for specimens exposed in SO_2/O_2 were explained by the immobilization of the calcium impurities as $CaSO_4$.

This year the studies have been extended to 400 hours in air and 256 hours in SO_2/O_2. Results are presented in Table 2 and Figures 3 and 4. The solid line in the figures is a least-squares power law fit of the mean four-point bend-test strength, σ, as a function of the time (in hours), t, at 1370°C for samples oxidized in air:

$$\sigma(\text{MPa}) = 768 - 109\ t^{0.229} \qquad (2)$$

The parameters derived for Equation 2 were the same whether or not the data points for times longer than 144 hours were included in the least-squares analysis.

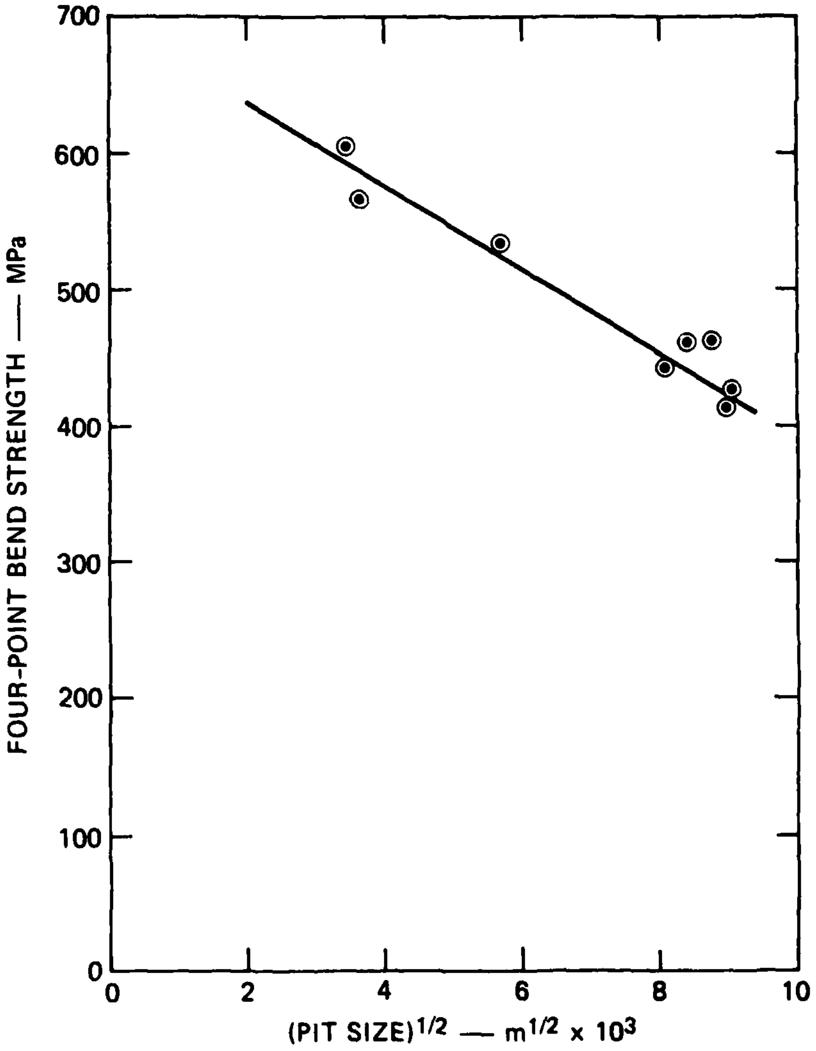

SA-5522-68

FIGURE 2 FOUR-POINT BEND STRENGTH OF OXIDIZED NC132 AS A FUNCTION OF SIZE OF PIT AT FRACTURE ORIGIN

Table 2

SUMMARY OF BEND-TEST RESULTS--BILLET 2

NC132 Test No.	History[a]	Bend Strength (MPa)
2-20	Unoxidized	768 ± 69
2-21	2-20 + 1370°C 4h in air	618 ± 61
2-28	2-20 + 1370°C 25h in air	537 ± 83
2-27	2-20 + 1370°C 144h in air	427 ± 83
2-25	2-20 + 1370°C 250h in air	418 ± 29
2-39[b]	2-20 + 1370°C 400h in air	300 ± 27
2-22	2-20 + 1370°C 64h in N_2	777 ± 70
2-23	2-20 + 1370°C 4h in O_2/SO_2	746 ± 26
2-29	2-20 + 1370°C 25h in O_2/SO_2	609 ± 30
2-24	2-20 + 1370°C 64h in O_2/SO_2	526 ± 54
2-30[b]	2-20 + 1370°C 144h in O_2/SO_2	327 ± 55
2-41[b]	2-20 + 1370°C 256h in O_2/SO_2	356 ± 45

---

[a] Treatment of the longitudinally ground samples.
[b] New data.

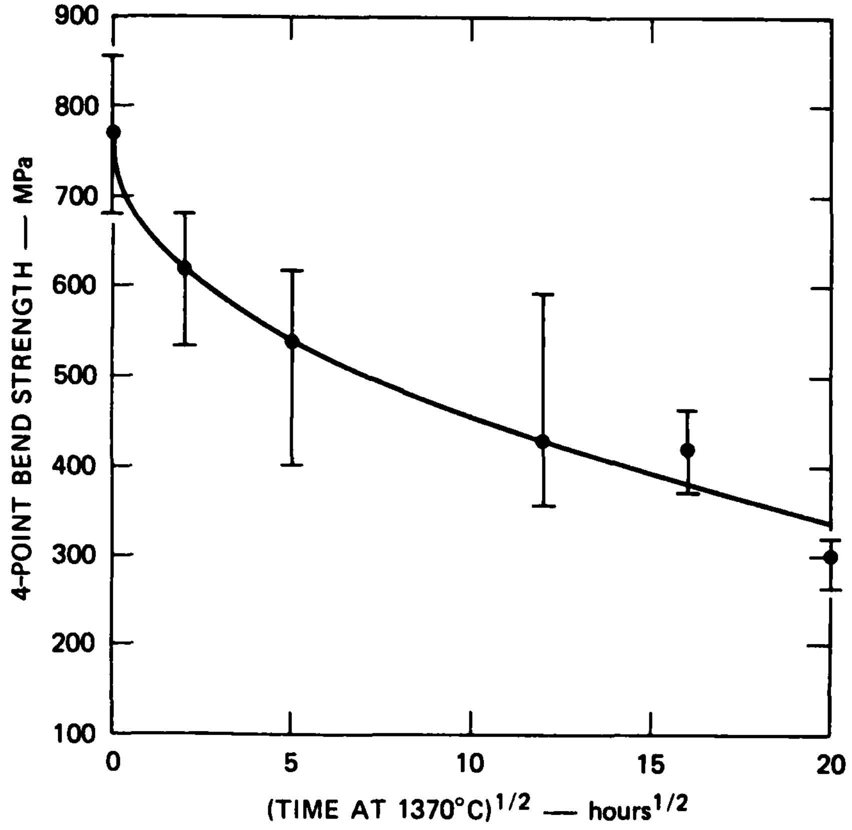

SA-5522-88

FIGURE 3 FOUR-POINT BEND STRENGTH OF NC132 SPECIMENS OXIDIZED IN AIR AT 1370°C

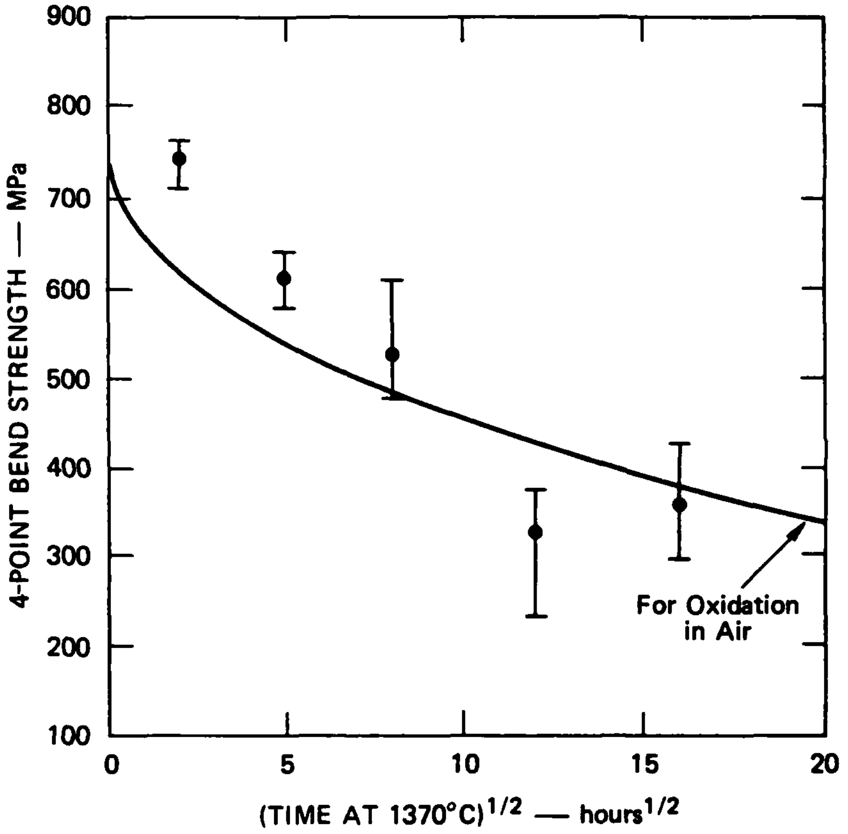

SA-5522-89

FIGURE 4 FOUR-POINT BEND STRENGTH OF NC132 SPECIMENS OXIDIZED IN 50 vol % SO_2/50 vol % O_2 AT 1370°C

Data for 400-hour exposure in air at 1370°C indicate that the strength of specimens continues decreasing at long exposure times, but at a lower rate than for short-term exposure.

Although the strength of NC132 specimens oxidized in SO_2/O_2 at 1370°C for up to 64 hours was greater than that of specimens oxidized under the same conditions in air, when oxidized for 256 hours, the strenth of both sets of specimens was essentially the same. The lower rate of degradation of the strengths of specimens oxidized up to 64 hours in SO_2/O_2, compared to the rate of those oxidized in air, was explained by the reaction

$$CaO(s) + SO_2(g) + \tfrac{1}{2}O_2(g) = CaSO_4(s) \qquad (3)$$

The product of this reaction has a low solubility in the silicate scale. The formation of $CaSO_4$ is most likely at the start of oxidation, when little SiO_2 is present. As SiO_2 is formed by the oxidation of Si_3N_4, calcium silicate-forming reactions become possible. For example, the reaction

$$CaSO_4 + CiO_2 = CaSiO_3 + SO_2 + \tfrac{1}{2}O_2 \qquad (4)$$

is thermodynamically favorable at 1370°C. Thus, the presence of SO_2 in the reaction gas could at first immobilize calcium as $CaSO_4$, which then reacts by slower, solid-state reactions with SiO_2 to form calcium silicates. Once the calcium is present as silicates, the tendency for pitting and strength degradation is equivalent in So_2/O_2 and in air.

EFFECT OF STRESS ON OXIDATION

Magnesia hot-pressed silicon nitride ceramics are known to creep under stress[6] at high temperatures. Since creep and oxidation are related to the properties of the intergranular phase, an investigation of the effect of stress on oxidation was made. Bend-test specimens were placed in a 4-point bend-test apparatus constructed of silicon carbide and heated in air for 64 hours at 1370°C under 4-point bending stresses of 57 and 113 MPa. The two specimens oxidized under stresses of 113 MPa had (weight gain/area)^2 values of 171 and 186 g^2/m^4. These values are 17 and 27% greater than those taken from the solid line of Figure 1 for unstressed oxidation in the air for the same time. The specimen oxidized under a stress of 57 MPa had a weight gain of 173 g^2/m^4, 18% greater than that for Figure 1.

The room temperature bend strengths of the specimens were 351 and 317 MPa for the bars oxidized under an applied stress of 113 MPa, and 265 MPa for the bar oxidized under a stress of 57 MPa. Although these strength determinations are less accurate than for unstressed samples (because of the slight deformation of the bars during oxidation), it is apparent that stress during oxidation drastically accelerates the degradation of the strength of NC132.

Both the increased rate of oxidation and the decreased room temperature strength of NC132 specimens oxidized under stress are understandable in terms of the mechanism of creep for MgO hot-pressed Si_3N_4, as discussed by Kossowsky et al.,[9] who showed that deformation of this material at high temperature took place by the mechanism of grain boundary sliding. As a result of creep deformation, wedge cracks open at grain junctions. The disruption of the boundary phase is sufficient to explain both the enhanced oxidation and decreased strength observed.

ELECTRON MICROPROBE STUDIES

In the first Interim Report,[1] we presented microprobe studies of NC132 bend-test specimens oxidized in air for 8 hours at 1400°C and for 40 Hours at 1371°C. During the past year we conducted similar investigations on cross sections of NC132 specimens oxidized at 1370°C for 144 hours in air and in a 50 vol% SO_2/50 vol% O_2 mixture. The results are shown in Figures 5 and 6.

The most important result of these experiments is the depletion of magnesium in the bulk of the ceramic, down from ~ 0.5-0.8 wt% in the as-received material to ~ 0.2 wt%. (Because this depletion results from diffusional processes, the extent would of course vary with specimen thickness.) The change in the magnesium concentration of the grain boundary phase is significant for several reasons.

(1) The slowing of the oxidation rate for long time exposure (see Figure 1) results from a lower magnesium gradient in the ceramic.

(2) A magnesium concentration that optimizes densification during hot pressing can be altered to improve mechanical properties and oxidation resistance by removing Mg during preoxidation prior to surface finishing.

(3) Because of the lower concentration, and the lower concentration gradient, of Mg and impurities in specimens preoxidized before surface grinding, pitting during subsequent oxidation will be decreased.

Calcium was found to concentrate in the oxide scale in a manner similar to Mg. Only 0.04 wt% of sulfur was found in the bulk of specimens oxidized in air or in SO_2/O_2. Apparently the sulfur found in the scale of the latter sample did not penetrate into the body of the ceramic.

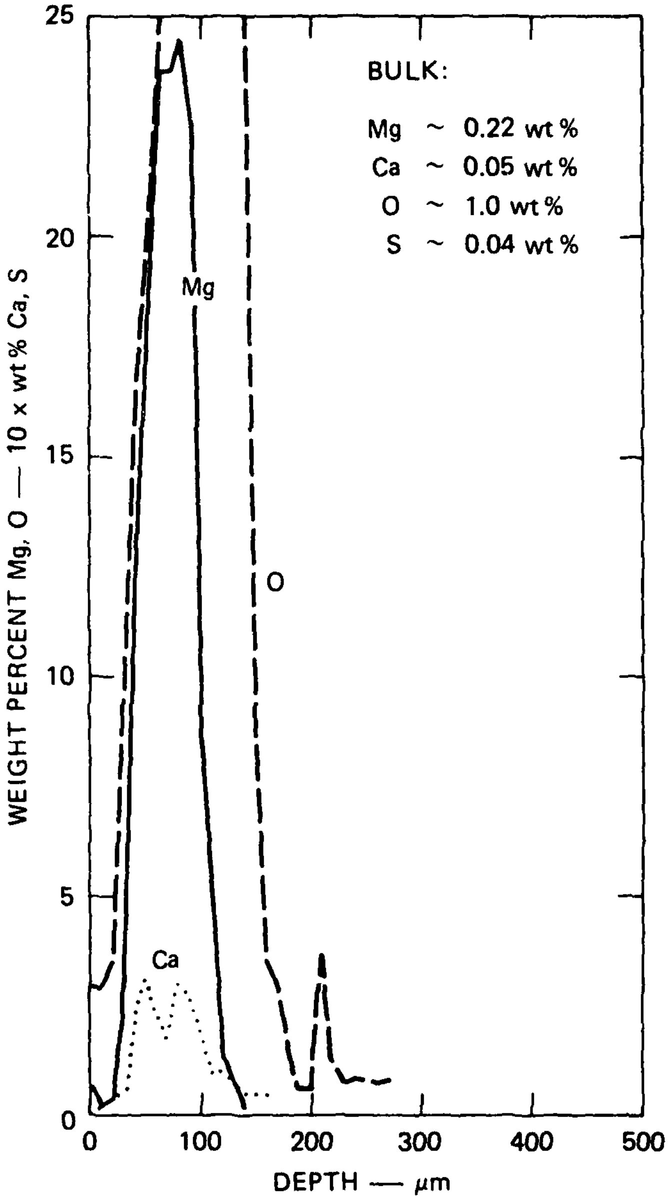

SA-5522-85

FIGURE 5 ELECTRON MICROPROBE TRACES OF A CROSS SECTION OF AN NC132 SPECIMEN OXIDIZED 144 HOURS IN AIR AT 1370°C

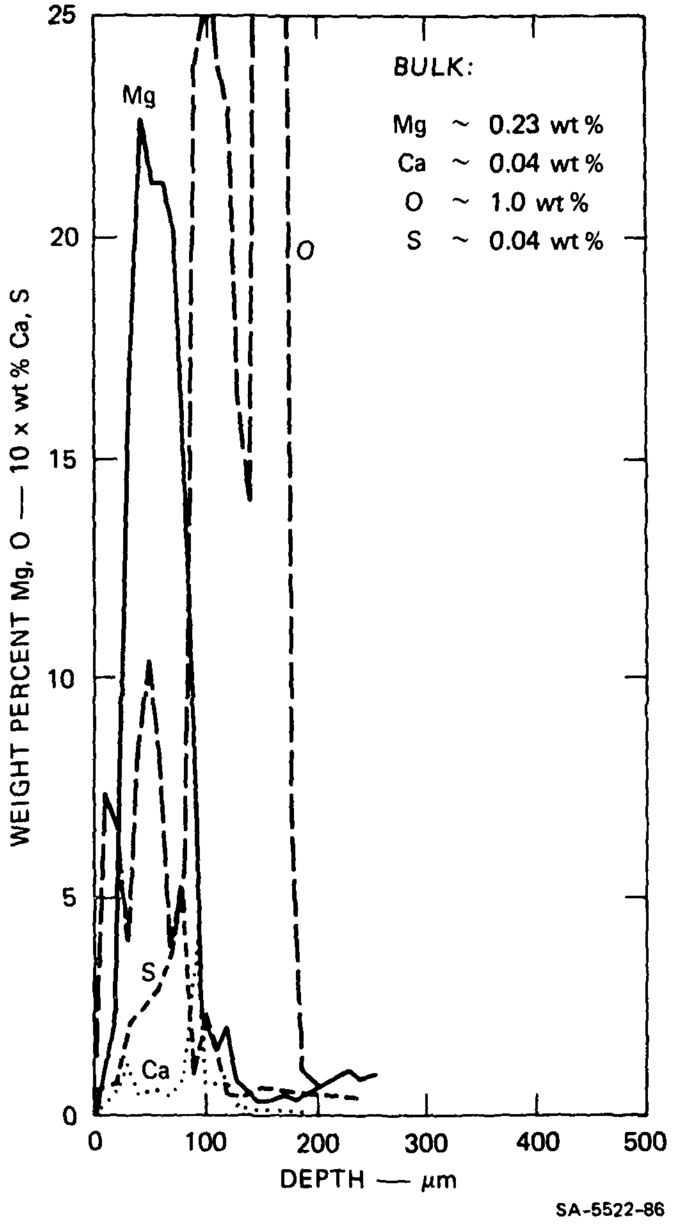

FIGURE 6 ELECTRON MICROPROBE TRACES OF A CROSS-SECTION OF AN NC132 SPECIMEN OXIDIZED 144 HOURS IN 50 vol% SO_2/50 vol% O_2 AT 1370°C

PITTING STUDIES

A major problem in the use of NC132 for high-temperature applications such as turbine parts is the formation during oxidation of strength-controlling pits at the oxide-substrate interface. The pits, which reduce the low- and intermediate-temperature fracture strength by acting as stress concentrators, decrease the ability of the ceramic to withstand the high stresses during the startup and shutdown, which can maximize at temperatures well below normal engine operating values.

The mechanism of pit formation in NC132 is related to the mechanism for oxidation.[1,2,3] The rate-controlling step in oxidation is the diffusion of magnesium through the silicate material in the grain boundaries of the ceramic into the oxide layer. The major oxidation process occurs in the oxide layer. Silicon nitride dissolves in the oxide, which is largely a silica silicate slag. The N^{-3} ions dissolved in the oxide are oxidized to N_2, which generates bubbles in the corrosion layer. The key role of magnesium is that the solubility of Si_3N_4 in the silicate slag is increased by the presence of MgO or other alkaline oxides.[10]

Since the concentration of Mg in the ceramic increases with depth, local incursions into the bulk will encounter a higher Mg concentration than at the planar interface. The ability to dissolve Si_3N_4 will be enhanced at local incursions, leading to accelerated local penetration of the oxide scale, and, eventually, to the formation of pits. The tendency to pit may be decreased by eliminating causes of local incursions, or by decreasing the subsurface magnesium gradient. Our experiments with surface contaminants investigated possible causes of the local incursions.

Our examination of strength-determining oxidation pits in broken NC132 bend-test specimens had found significant amounts of Ca and lower amounts of Mg than the average for the scale.[3] This observation did not indicate whether the Ca caused the pit to be formed, or whether the Ca was simply what remained after pit formation and fracture of the test specimen. We undertook a series of tests in which known contaminants were placed on the surface of bend-test bars to check their tendencies to increase the local rate of attack.

The surface contaminants used were those found as impurities in NC132 (CaO, MgO, MnO, Fe, CoO, Al_2O_3, W, WC), substances found in the oxidized scale (SiO_2, diopside = $CaMgSi_2O_6$), and Na_2SO_4. In several instances, carbonates were utilized instead of oxides. Since the carbonates dissociated to oxides upon heating, this did not influence the results. The contaminants were attached to the ceramic with melted parafin, which vaporized upon heating. The Na_2SO_4-doped specimens were exposed in air at 1000°C for 64 hours. Half of the Na_2SO_4 samples were then exposed in air for 64 hours at 1370°C. All the other specimens were exposed for 4 or 64 hours in air at 1370°C. Specimens were broken in a 4-point bending jig after exposure, and were examined by either optical microscopy or SEM.

Weight gain measurements of test specimens did not prove useful, since weight changes caused by small quantities of dopant were unmeasurable, and larger quantities of dopant tended to spall off during heating and cooling.

At first, small quantities (~ 40 μm diameter) of contaminants were placed at sites in the middle of the bend test bars in the zone where fracture should occur in subsequent bend tests. However, fracture origins did not coincide with the contaminant sites, indicating that pits produced in this way were not more severe than those developed during oxidation of clean-surfaced NC132. In subsequent experiments, light coatings of powdered contaminant were distributed as evenly as possible over the central portion of the specimens. These conditions led to a more general attack on the ceramic, rather than the development of specific pit sites.

Optical microscopy and SEM examinations revealed that the degree of attack on the ceramic varied considerably according to the contaminant species. The dompants were separated into three qualitative categories, dopant causing moderate, severe, and very severe damage.

Moderate damage:	MgO, SiO_2, W, WC
	Al_2O_3, CoO, MnO
Severe damage:	Fe, CaO
Very severe damage:	Na_2SO_4, diopside

Moderate damage was characterized by some attack on the ceramic beneath the oxide scale, but the surface of the ceramic remained essentially planar with minor local incursions. Damage was considered severe if local erosion of ~ 50 μm depth was visible under the optical microscope. Damage was considered very severe if extensive areas of erosion, from ~ 80-100-μm in depth, were observed. The effect of these contaminants on the strength of Si_3N_4 after oxidation was also examined for a limited number of specimens. The strength data are listed in Table 3. Although the degradation of strength follows the order of severity of attack to some degree, these strength results are very much influenced by the random, nonuniform nature of the contaminant particles and are less reliable indicators of reactivity with HC132 than the microscope examinations noted above.

The ability of elemental iron to induce oxidation pits in NC132 was reported by Lange.[11] The degradative effects of Na_2SO_4 and Na_2O on Si_3N_4 have been reported by Browne and Tressler[12] for MgO hot-pressed material, and by Levy and Falco[13] and Mayer and Riley[14] for reaction-bonded Si_3N_4. The enhanced reactivity associated with these impurities has been attributed to the presence of liquid silicate phases,[15] which can provide more rapid chemical transport than solid phases and may have larger Si_3N_4 solubilities than the solid silicate phase.

The presence of liquid phases associated with the presence of impurities is undoubtedly part of the mechanism of corrosion observed in these tests. Diopside, which liquefies below 1370°C for compositions in the silica rich portions of its phase field,[15] was more corrosive than CaO alone. The system FeO--MgO--SiO_2, however, has high-iron, high magnesia content liquid phases at this temperature,[16] but is less obviously corrosive than diopside. This is perhaps a result of the more basic character of CaO, which promotes dissolution of nitride in silica slags, while FeO does not.

Table 3

FOUR-POINT BEND STRENGTHS OF NC132 SPECIMENS AFTER OXIDATION IN AIR

Test No.	Dopant	History	Bend Strength (MPa)
2-33A	Na_2SO_4	25h, 1000°C	242 ± 22
2-33B	Na_2SO_4	2-33A + 64h, 1370°C	276[a]
2-34 (1,2,9)	$CaCO_3$	64h, 1370°C	433 ± 105
2-34(3,4,10)	$MgCO_3$	64h, 1370°C	456 ± 65
2-34 (5,6,11)	Fe	64h, 1370°C	454 ± 15
2-34 (7,8)	$CoCO_3$	64h, 1370°C	515 ± 18
2-34 (1)	$MgCO_3$	16h, 1370°C	386[a]
2-35 (2)	$CaCO_3$	16h, 1370°C	341[a]
2-43 (1-3)	diopside	64h, 1370°C	324 ± 16
2-43 (4-6)	SiO_2	64h, 1370°C	308 ± 31
2-43 (7-9)	MgO	64h, 1370°C	365 ± 12
2-44 (1-3)	$CaCO_3$	64h, 1370°C	420 ± 64
2-44 (4-6)	WC	64h, 1370°C	580 ± 58
2-45 (1-3)	SiO_2	4h, 1370°C	463 ± 15
2-45 (4-6)	$CaCO_3$	4h, 1370°C	372 ± 97
2-45 (7-9)	$MgCO_3$	4h, 1370°C	482 ± 30

---

[a] Single specimen

Our results indicate that in the manufacture of magnesia hot-pressed Si_3N_4 emphasis should be placed on the reduction of the impurities considered in this section. Of the species reported as present in NC132, calcium and iron appear to be the most serious contributors to the formation of pits.

REOXIDATION EXPERIMENTS

In the first Interim Report, we reported that the rates of weight gain during oxidation were essentially unaffected by removal of the oxide scale, and that grinding of the oxidized surfaces to remove scale and oxidation pits returned strengths to preoxidation values. To investigate these effects further, we oxidized twelve bend-tests bars for 144 hours at 1370°C in air (preoxidation) and removed the oxide scale. Four of the bars were then broken in the bend-test apparatus. The remaining eight were oxidized 144 more hours at 1370°C in air (reoxidation). Four of these bars were then broken as oxidized, and four were surface-ground and broken.

As expected, the weight gain was smaller during the second oxidation than during the first, (see the open triangle in Figure 1). The effects of these procedures on strength are shown in Figure 7. The strengths of specimens ground after oxidation are comparable to those of unoxidized specimens. Specimens oxidized 144 hours, ground, reoxidized 144-hours, then broken without further surface finishing had strengths comparable to those of NC132 specimens after a single oxidation of about 40 hours.

Oxidation surfaces of specimens that had been broken in four-point bend tests were examined metallographically. The degree of surface pitting of samples ground after 144 hours preoxidation in air at 1370°C and reoxidized 144 hours in air at 1370°C was considerably reduced over samples oxidized without preoxidation and grinding, as shown in Figure 8. Because pitting is related to the magnesium gradient, development of pits after preoxidation (to lower the magnesium gradient) and surface grinding was expected to be much slower than in NC132 as received. This is exactly what was observed in these experiments.

Further insight into the course of oxidation in NC132 was gained by consideration of the densities of the reoxidation specimens. Densities for specimens as received or ground to remove oxidation scale were (grams/cm^3):

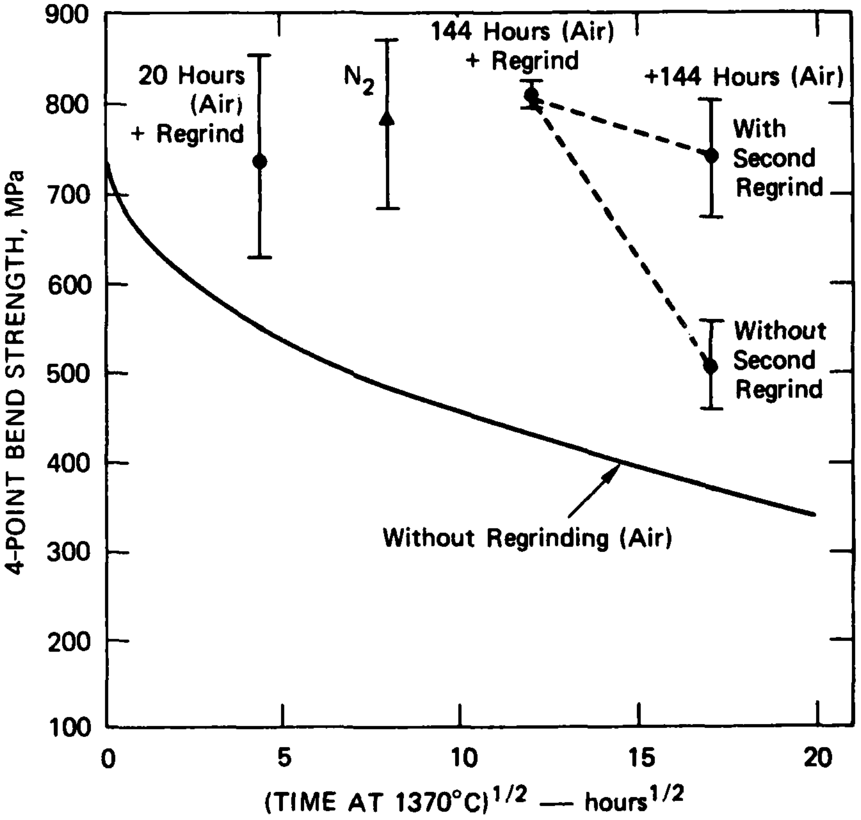

SA-5522-90

FIGURE 7 STRENGTH OF NC132 SPECIMENS OXIDIZED IN AIR AND IN N_2 AT 1370°C — EFFECT OF SURFACE FINISHING ON STRENGTH

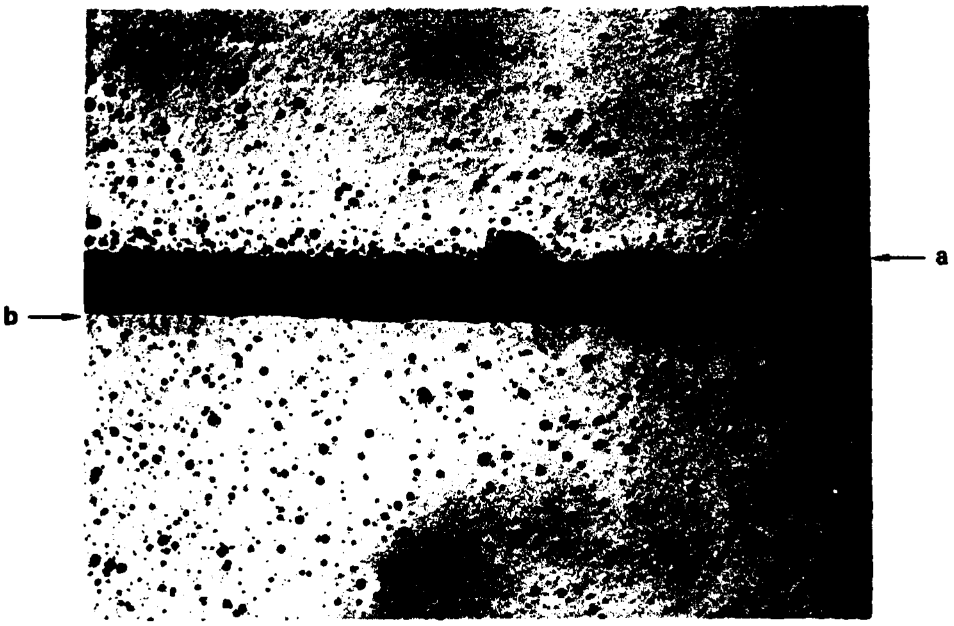

SA-5522-91

FIGURE 8 CROSS SECTIONS OF NC132 SPECIMENS OXIDIZED IN AIR AT 1370°C

The oxide scales were lost during polishing (width of photograph = 1.1 mm).

(a) Oxidation surface of as-received NC132 after 144 hour exposure.

(b) Oxidation surface of sample preoxidized 144 hours, surface-ground, and reoxidized 144 hours.

NC132 as received	3.20
After 144 hours at 1370°C, reground	3.12
After additional 144 hours at 1370°C and second regrinding	3.14

In the first 144 hours the density decreased because of transfer of Mg into the oxide scale. During the second 144 hours less Mg was transferred to the scale, and some weight was gained, presumably by oxygen transport along grain boundary phases.

SUGGESTIONS FOR FUTURE WORK

The most important result of the oxidation studies on NC132 has been the elucidation of the relationship between oxidation of Si_3N_4 and the properties of the intergranular Mg-containing phase.

The most promising future work on NC132-type materials, in our opinion, will be studies in which hot-pressed material is oxidized to adjust the Mg content of the intergranular phase to improve the high-temperature-strength, creep resistance, and oxidation resistance. Preoxidation followed by surface finishing will lower the Mg content of the ceramic and remove most of the calcium impurity. These procedures should reduce the rate of formation of strength-limiting oxidation pits. Thus, preoxidation of as-received NC132 should produce a material with better oxidation resistance and improved mechanical properties for high-temperature applications.

REFERENCES

1. D. Cubicciotti, K. H. Lau, and R. L. Jones, SRI Interim Report 5522-1, Contract F44620-76-0116 (November 1977).

2. D. Cubicciotti, K. H. Lau, R. L. Jones, and D. J. Rowcliffe, SRI Interim Report 5522-2, Contract F44620-76-C-0116 (November 1978).

3. D. Cubicciotti, K. H. Lau, D. J. Rowcliffe, and R. Lamoreaux, SRI Interim Report 5522-3, Contract F44620-76-C-0116 (November 1979).

4. D. D. Cubicciotti, R. L. Jones, and K. H. Lau, J. Electrochem. Soc. 124, 1955 (1977).

5. D. D. Cubicciotti and K. H. Lau, J. Am. Ceram. Soc. 61, 512 (1978).

6. J. A. Palm and C. D. Greskovich, Am. Ceram. Soc. Bull. 59, 447 (1980).

7. JANAF Thermochemical Tables, NSRDS-NBS 37, (U.S. Government Printing Office, Washington, D.C., 1971, and supplements)

8. I. Barin and O. Knacke, Thermochemical Properties of Inorganic Substances (Springer-Verlag, Berlin and New York, 1973).

9. R. Kossowsky, D. G. Miller, and E. S. Diaz, J. Mater, Sci. 10, 983 (1975).

10. E. A. Dancy and D. Janssen, Can. Metall. Q. 15, 103 (1976).

11. F. F. Lange, J. Am. Ceram. Soc. 61, 270 (1978).

12. W. C. Browne and R. E. Tressler, Am. Ceram. Soc. Bull. 59, 443 (1980).

13. M. Levy and J. J. Falco, Am. Ceram. Soc. Bull. 57, 457 (1978).

14. M. I. Mayer and K. L Riley, J. Mater. Sci. 13, 1319 (1978).

15. E. M. Levin and H. F. McMurdie, Phase Diagrams for Ceramists (American Ceramic Society, Columbus, Ohio, 1975).

16. E. M. Levin, C. R. Robbins, and H. F. McMurdie, Phase Diagrams for Ceramists (American Ceramic Society, Columbus, Ohio, 1964).

Appendix B

KINETICS OF OXIDATION OF CHEMICALLY VAPOR-DEPOSITED SILICON NITRIDE

by

R. H. Lamoreaux, K. H. Lau, and D. D. Cubicciotti

(As submitted to the Journal of the Electrochemical Society)

Appendix B

KINETICS OF OXIDATION OF CHEMICALLY VAPOR-DEPOSITED SILICON NITRIDE

R. H. Lamoreaux, K. H. Lau, and D. D. Cubicciotti
SRI International, Menlo Park, California 94025

ABSTRACT

The oxidation of CVD silicon nitride from three sources was measured thermogravimetrically at temperatures from 1380 to 1818 K in 20 kPa of dry oxygen for times to about 25 hours, and in air at 1372 K for 81 hours. Oxidations become parabolic after an initial period of high weight gain, which was associated with oxidation along pores that became closed off by the reaction product. Above 1725 K, oxidation rates increased more rapidly with temperature for several specimens. Specimens were examined by electron microprobe and scanning electron microscope techniques. Oxidation rates for CVD Si_3N_4 were compared with those for two grades of hot-pressed Si_3N_4, powdered Si_3N_4, and silicon. A mechanism for the increased reaction rate above 1725 K is proposed.

Key words: ceramics, corrosion refractories.

INTRODUCTION

Silicon nitride is a promising material for use in high temperature applications because of its high temperature strength and corrosion resistance. Information about the fundamental oxidation properties of the various forms of silicon nitride (hot-pressed, sintered, reaction-bonded, and chemically vapor-deposited) can aid in the development of dense silicon nitride materials with improved performance.

We have previously investigated the oxidation of Si_3N_4 hot-pressed with magnesia,[1] and with yttria,[2] as densification aids. The densification aids were found to participate in the mechanism of oxidation for both materials. The present studies were undertaken to determine the oxidation behavior of compact bodies of chemically pure Si_3N_4, and to establish base line information for the oxidation of hot-pressed material.

Previous studies of the oxidation of pure Si_3N_4 include measurements on powdered samples by Horton,[3] Mukerji and Nandi,[4] Fitzer and Ebi,[5] and by Tetard et al.[6] Of these measurements, only Tetard et al. accounted for the reaction area that changed significantly during oxidation. Previous oxidation studies on chemically vapor-deposited (CVD) Si_3N_4 were the very limited measurements of Rosolowski and Greskovich,[7] Franz and Langheinrich,[8] and Galasso.[9] These studies were in poor agreement with each other, indicating the need for further investigation.

EXPERIMENTAL

Samples. Three sources donated samples of experimentally produced CVD silicon nitride:

(a) Chemetal Corporation samples were furnished deposited on graphite substrates, which were removed by burning in air for 10 hours at 1273 K. Some oxidation of CVD material occurred in this procedure. The resulting samples were flat, 0.15 to 0.45 mm thick, light tan in color, and rough-surfaced.

(b) General Electric Company specimens were irregularly shaped, flat, black-brown pieces about 0.012 cm thick, and smoother than the other samples.

(c) United Technologies samples were fracture pieces 0.8 to 1.2 mm in wall thickness. The samples were either milky white or gray and rough-surfaced.

X-ray diffraction patterns of unoxidized material from each source showed only lines for α-Si_3N_4, although amorphous material might have been present. The surface roughness precluded accurate evaluation of reaction areas, which were too small for BET evaluation. The areas used for calculations ignored roughness, actual areas could have been greater by as much as a factor of 3. The variations in surface morphology and color are attributable to the particular deposition conditions involved. Tanzilli et al.[10] reported that the oxygen content of white CVD Si_3N_4 was high (~ 1.4 wt%), whereas that of brown CVD Si_3N_4 was low (~ 0.4 wt%).

Thermogravimetric Studies. Suspension holes of 0.1 cm diameter were ultrasonically drilled in each specimen. The specimens were suspended by 0.025-cm-diameter sapphire rods in the thermogravimetric apparatus, which has been previously described.[2] Oxidations were performed in 20 kPa (150 torr) of dry O_2 under the time and temperature conditions given in Table I. Several oxidations done in air are also included in the table. Specimens CM-2 and UT-1 were oxidized, cooled to room temperature, and reoxidized. Specimens UT-2 and UT-3 were oxidized at two different temperatures without intermediate cooling. Weight gains were continuously recorded except for UT-3 at 1343 K, for which only measurements of the total weight gain were obtained because of balance problems, and for UT-4, which was oxidized in air for 81 hours at 1327 K.

Results. Total weight gains for each oxidation stage are shown in Table I, and plots of (weight gain/area)^2 versus time are shown in Figures 1-3. We believe that the high initial rate of oxidation resulted from pores and grain boundaries that were sealed off by the oxide formed during the oxidation (see below).

For the majority of specimens, the weight gain became parabolic after an initial period. The exceptions were the results of Figure 2 and the result for UT-1 at 1748 K in Figure 3. The curve for GE-1, oxidized at 1739 K, showed a hump at about 6 hours but otherwise was parabolic. Specimens GE-2 and GE-3 did not exhibit well-defined parabolic behavior even for large total weight gains. Data for the parabolic oxidation regions of all specimens, including those that were only approximately parabolic, were least-squares fitted to yield the dashed lines shown in Figures 1-3 and the parabolic oxidation constants of Table I. For two specimens--UT-3 at 1343 K, and UT4, only total weight gains were available; rate constants for these were estimated by assuming parabolic kinetics throughout the oxidations.

SEM Examinations. Scanning electron microscope (SEM) examinations of unoxidized samples revealed the roughness (Figure 4), which precluded evaluation of surface areas, and a columnar grain structure with intergranular pores in the subsurface material (Figures 4 and 5). Apparently oxidation takes place on these pore surfaces until the surface oxide layer closes them off, as seen in Figure 6.

Figure 7 shows the adherent, protective scale formed by oxidation in air for 81 hours at 1327 K. For oxidations at temperatures above about 1725 K, distinct boundaries between the scale and the substrate became evident, as seen in Figures 6 and 8. These two figures show the surfaces of specimens that were oxidized, cooled to room temperature, and reoxidized. The latter oxidation in Figure 6 and both oxidations in Figure 8 were done above 1725 K; only one oxide layer is seen in Figure 6, whereas two layers are evident in Figure 8.

Figures 9a through 9d show a taper-ground section of the specimen oxidized 8 hours at 1818 K, the highest temperature of the present study. Figure 9a shows the unattacked subsurface region on the left, and a porous subscale region on the right. Figure 9b shows this porous region on the left, and the unground surface on the right. The oxide layer flaked off during the sectioning. The unground surface with part of the oxide layer still attached is seen in Figure 9c, and in higher magnification in Figure 9d.

Electron Microprobe Analyses. Electron microprobe analyses were made of polished cross sections of specimens UT-1 (oxidized 22 hours at 1385 K and 19 hours at 1748 K) and UT-2 (oxidized 14 hours at 1482 K and 14 hours at 1711 K). The concentration profiles of O, Si, and N through the cross sections are shown in Figures 10 and 11. Specimen UT-1, the more severely oxidized specimen, shows significant oxygen content to a depth of about 100 μm; this is well below the surface layer of oxide, which was less than 20 μm.

DISCUSSION

Oxidation Products. Oxidized samples were examined by x-ray diffraction. Cristobalite and α-Si_3N_4 lines were found, but there was no evidence of silicon oxynitride. In most instances the silica scale thickness observed by SEM was consistent with the total weight gain according to the equation.

$$Si_3N_4(s) + 3O_2(g) \rightarrow 3SiO_2(s) + 2N_2(g) \qquad [1]$$

In certain instances the oxide scale was not thick enough to account for the total weight gain (for example, UT-1 in Table I and Figure 6). In these instances the weight gain must have involved dissolution of oxygen in the α-Si_3N_4 lattice and oxidation along interior pores. (Homogeneous α-Si_3N_4 phases with 1.5 wt% oxygen have been reported,[11] and microprobe analysis showed high oxygen levels in the interior of UT-1).

Comparison of Results with Literature Values. Tetard et al.[6] studied the oxidation rates of two lots of Si_3N_4 powder (with ratios of α to β crystal forms of 2.0 and 1.4) in 4 kPa (30 torr) of dry O_2 from 1373 to 1573 K, taking the change of surface area measured by the BET method during oxidation into account. On the basis of these measurements, they postulated three sequential reaction regimes for the oxidation of chemically pure Si_3N_4: (a) a short region of chemisorption of oxygen on the Si_3N_4 surface, (b) a region of linear reaction kinetics, and (c) a region of parabolic oxidation kinetics controlled by the diffusion of oxygen through the silica scale. The latter two regimes correspond to the linear-parabolic oxidation kinetics proposed by Deal and Grove[12] for silicon.

We were unable to determine the reaction kinetics for CVD Si_3N_4 during the early stages of oxidation, because the reaction area changed as pores and grain boundaries were sealed off by the growing oxide layer. The parabolic oxidation constants for powdered[6] and CVD[7,9] silicon nitride, and for silicon[12] are shown in the Arrhenius plot of Figure 12. The data for powdered Si_3N_4 and silicon were treated as discussed in the Appendix to put them on comparable weight gain bases with CVD Si_3N_4. The parabolic rate constants of the present study are consistent with the value of Galasso,[9] but are higher than the results of Rosolowski and Greskovich.[7] Considering the probable differences in the ratio of actual to nominal reaction area, different conditions of oxidation, and the exaggeration of experimental differences by the squared term (weight gain/area)^2, the results are reasonably consistent.

The parabolic oxidation constants of the present study were least-squares fitted to the equation

$$\log K = a + b\, T^{-1} \qquad [2]$$

where K is the parabolic weight gain constant and T is the absolute temperature; the result was the line through the data points shown in Figure 12. The activation energy (= -2.303 R b) for parabolic oxidation was 25.6 kcal/mole. This is in good agreement with the value of 28.5 kcal/mole for the parabolic oxidation of silicon in dry O_2,[12] and with Norton's[13] value of 27.0 kcal/mole for the activation energy of oxygen diffusion in fused silica. The three points marked with asterisks in Figure 12 were not included in the least-squares analysis for reasons noted below. If they had been included, the activation energy for parabolic oxidation of CVD Si_3N_4 would have been 33.5 kcal/mole. The absolute values of the parabolic oxidation constants are roughly eight times those for silicon at equal temperatures If the actual surface areas of the CVD Si_3N_4 samples were ~ three times the nominal areas, the parabolic oxidation rates would be equivalent. We believe the close agreement of both rate constants and activation energies between CVD Si_3N_4 and silicon indicates that diffusion of oxygen through the oxide layer is rate controlling in the parabolic oxidation region.

Tetard et al.[6] measured the parabolic oxidation rates of two lots of Si_3N_4 powder, lot A with an α/B ratio of 2:1, and lot B with $\alpha/B = 1.4$. The rate constants were calculated using areas determined by the BET technique as a function of the extent of oxidation; those for lot A were about three times greater than those for lot B. They concluded that α-Si_3N_4 was more reactive than β-Si_3N_4. This conclusion is not consistent with oxygen diffusion through the silica layer being the rate determining process in the parabolic oxidation of Si_3N_4. Another explanation for the different reaction rates of the two powder lots is a difference in surface configuration beneath the growing oxide scale. The results for both lots of Si_3N_4 powder lie for the most part between the present results for CVD Si_3N_4 and the extrapolated values for silicon; the differences in parabolic rate constants for the oxidation of powdered Si_3N_4, CVD Si_3N_4, and silicon lie within the uncertainties in reaction surface areas.

High Temperature Oxidation. Several oxidations of CVD Si_3N_4 above about 1725 K exhibited high weight gain and only approximately parabolic kinetic behavior, even for large values of the total weight gain. These phenomena imply a change in the rate-limiting mechanism of oxidation: the nature of the silica scale changed either by an internal phase transformation or by a mechanical disruption.

The equilibrium phase of silica from 1400 to 1743 K is tridymite; above 1743 K cristobalite is the stable form.[14] A large amount of evidence indicates that this phase transition was not the primary reason for the increased oxidation rates. In the present study the only crystalline silica product observed by x-ray diffraction after oxidation at temperatures below 1743 K was cristobalite, as found by Rosolowski and Greskovich[7] for oxidation of CVD Si_3N_4 at 1683 K. Cristobalite was also the crystalline silica form found on oxidized powdered Si_3N_4 by Mukerji and Nanid,[4] and by Fitzer and Ebi,[5] although Tetard et al.[6] could not distinguish between cristobalite and tridymite, and Horton[3] found tridymite. When cristobalite is formed at lower temperatures, the tridymite-crystobalite transition will not bring about a breakdown of the protective silicon scale.

Further evidence that this phase transition is not the predominant factor in the rapid high temperature oxidation of Si_2N_4 is seen in Figure 13. The changes in slope of the lines for oxidation of yttria[2] and magnesia[15] hot-pressed, and for powdered[5] Si_3N_4, occur in the same temperature region as for the CVD material. The oxide scale on the magnesia hot-pressed Si_3N_4 has been shown to be nonprotective,[1] and that on the yttria hot-pressed material only somewhat protective.[2]

Therefore, a crystal phase transformation in these scales could not account for the increased oxidation rates.

A more probable explanation for the increased oxidation above about 1725 K is, in our opinion, the existence of a secondary reaction that becomes thermodynamically favored at these temperatures. Although we have no proof, the following process is consistent with all observations: the reaction

$$2Si_3N_4(s) + SiO_2(s) = 2Si_2ON_2(s) + Si(\ell) + 2N_2(g) \qquad [3]$$

has an equilibrium nitrogen pressure indicated by the dashed lines in Figure 13. (The data used to calculate the equilibrium pressure are summarized in the Appendix.) In the temperature range where there is a transition to higher rate constants (above 1725 K), the pressure of N_2 from Reaction [3] becomes large enough to produce significant mechanical effects. The scale could break down entirely at (random) times. Such a process could explain the curves of Figure 2. Silicon oxynitride, Si_2ON_2, has been observed as an oxidation product in both MgO and Y_2O_3 hot-pressed Si_3N_4. We did not detect its presence (by x-ray diffraction) in oxidized CVD Si_3N_4; however, only a thin layer of the oxynitride would be needed to produce nonadherence.

REFERENCES

1. D. D. Cubicciotti and K. H. Lau, J. Amer. Ceram. Soc. 61, 512 (1978).

2. D. Cubicciotti and K. H. Lau, J. Electrochem. Soc. 126, 1723 (1979).

3. R. M. Horton, J. Amer. Ceram. Soc. 52, 121 (1969).

4. J. Mukerji and A. K. Nandi, Indian J. Technol. 16, 419 (1979).

5. E. Fitzer and R. Ebi, Silicon Carbide--1973, (R. C. Marshall et al., Eds.) University of South Carolina Press, Columbia, SC (1974), p. 320.

6. D. Tetard, P. Lortholary, P. Goursat, and M. Billy, Rev. Int. Haut. Temp. Refrac. 10, 153 (1973).

7. J. H. Rosolowski and C. D. Greskovich, "Ceramic Sintering," Semi-annual Technical Report, ARPA Order No. 2698, Program No. 4D10, Advanced Research Projects Agency, Office of Naval Research, Arlington, Virginia (Oct. 1974).

8. I. Franz and W. Langheinrich, Solid-State Electronics 14, 499 (1971).

9. F. S. Galasso, Powder Met. Internat. 11, 7 (1979).

10. R. A. Tanzilli, J. J. Gebhard, J. D'Andrea, C. Dulka, J. Hanson, and R. Kreitz, "Processing Research on Chemically Vapor Deposited Silicon Nitride--Phase 2," General Electric Company Document No. 795 DR 2324 (1979), p. 3-1.

11. S. Wild, P. Grieveson, and K. H. Jack, Special Ceramics 5, (P. Popper, Ed.), British Ceramic Research Association, Stoke-on-Trent (1972) 385.

12. B. E. Deal and A. S. Grove, J. Appl. Phys. 36, 3770 (1965).

13. F. J. Norton, Nature 171, 701 (1961).

14. R. Kern and A. Weisbrod, Thermodynamics for Geologists, Freeman, Cooper, and Company, San Francisco (1967), p. 115.

15. W. C. Tripp and H. C. Graham, J. Amer. Ceram. Soc. 59, 399 (1976).

16. A. Hendry, NATO Adv. Study Inst. Ser., Ser. E. 1977, E 23 (Nitrogen Ceramics) 289.

ACKNOWLEDGMENTS

This research was sponsored by the Air Force Office of Scientific Research (AFSC), with Captain S. Wax as technical monitor, under Contract F44620-76-C-0116. The authors are indepted to Chemetal Corporation, The General Electric Company, and United Technologies for the CVD Si_3N_4 samples, and to Mr. J. Terry for the SEM work.

APPENDIX

A. Data Treatment for Figures 13 and 14.

All parabolic rate data were converted to SI units: $kg^2\ m^{-4}\ s^{-1}$,

CVD Si_3N_4. The total weight gain measurement of Galasso[9] was used to derive a rate constant by assuming parabolic kinetics throughout the oxidation. The thin film thickness measurements of Franz and Langheinrich[8] did not allow calculation of weight gains, since oxygen dissolved in α-Si_3N_4 was not measured.

Powdered Si_3N_4. The studies of Horton,[3] Mukerji and Nandi,[4] and Fitzer and Ebi[5] did not take account of the change in reaction area during oxidation. These were omitted from Figures 12 and 13 except that the data of Fitzer and Ebi, which indicated a change in oxidation mechanism above about 1700 K, were included in Figure 13.

Tetard et al.[6] used BET measurements to determine reaction areas as a function of the extent of reaction. They derived the following expression for the linear-parabolic oxidation kinetics of powdered Si_3N_4:

$$x + \frac{K_D}{K_R} x = K_D t \qquad [A-1]$$

where x is the oxide film thickness, K_D and K_R are the parabolic and linear rate constants, respectively, and t is the oxidation time. Deal and Grove[12] had derived an equivalent equation for the linear-parabolic oxidation of silicon. Tetard et al. then took the oxide film thickness

x_i at some time t_i in the linear-parabolic region, and the film thickness x at some later time t, and substituted these values in Equation [A-1] to derive the expression

$$x-x_i = \left[\frac{t-t_i}{x-x-_i} - \frac{1}{K_R} \right] K_D \qquad [A-2]$$

This expression does not follow from [A-1]. The correct expression is

$$x+x_i = \left[\frac{t-t_i}{x-x_i} - \frac{1}{K_R} \right] K_D \qquad [A-3]$$

We have recalculated the K_D values of Table II of Tetard et al. using their values of x_i and t_i, values of K_R from their Table I, and points taken at x, t from the curves of their Figures 6 and 7. The results that apply to their experimental O_2 pressure (4 kPa - 30 torr) are shown in Table A-I. We have analyzed their data and concluded that their measurements of the pressure dependence of the oxidation rate were made in the linear kinetic region, where no pressure dependence is expected.[12] For Figure 13 the corrected values of Table A-I were multiplied by 5 to place them on a comparable basis.

Silicon. Because the weight gain in the reaction

$$Si(s, \ell) + O_2(g) \rightarrow SiO_2(s) \qquad [A-4]$$

is 32.0 g/mole SiO_2 and the weight gain in reaction [1] is 13.3 g/mole SiO_2, the parabolic oxidation constants of Deal and Grove[12] for dry O_2 were multiplied by $(13.3/32.0)^2$ after conversion to $kg^2\ m^{-4}\ s^{-1}$ units to place them on a comparable basis, and by (20/101.3) to normalize them to the 20 kPa O_2 pressure used in the present work.

B. Thermodynamic Data

Gibbs energies of formation for the evaluation of the equilibrium nitrogen pressure for Reaction [3] were taken from Hendry:[16]

$$\Delta G^\circ_f(\alpha\text{-}Si_3N_4) = -279.0 + 1.42 \times 10^{-1}\ T \text{ kcal/mole}$$

$$\Delta G^\circ_f(SiO_2) = -224.7 + 0.48 \times 10^{-1}\ T \text{ kcal/mole}$$

$$\Delta G^\circ_f(Si_2ON_2) = -157.3 + 0.31 \times 10^{-1}\ T \text{ kcal/mole.}$$

Table I: Sequential oxidation treatment of CVD specimens [CM = Chemetals Corporation, GE = General Electric Company, UT = United Technologies]

Sample	T, K	Time, Hours	Apparent Surface Area, $m^2 \times 10^4$	Weight Gain, $g \times 10^3$	Parabolic Rate Constants, k, $kg^2\ m^{-4}\ s^{-1}$
CM-1	1373	10[a]	20.30	b	b
	298			–	–
	1730	7		2.95	7.2×10^{-11}
CM-2	1373	10[a]	19.54	b	b
	298			–	–
	1751	8		3.32	8.14×10^{-11}
	298			–	–
	1787	5		0.85	8.52×10^{-11}
GE-1	1739	21	3.0	0.71	7.81×10^{-11}
GE-2	1795	6	1.7	0.28	4.6×10^{-10}[d]
GE-3	1818	8	1.7	0.33	5.1×10^{-10}[d]
UT-1	1385	22	7.73	1.12	1.47×10^{-11}
	298			–	–
	1748	19		2.39	2.28×10^{-10}[d]
UT-2	1482	14	5.35	0.59	1.93×10^{-11}
	1711	14		0.57	5.21×10^{-11}
UT-3	1343	28	4.91	0.52	1.11×10^{-11}[c]
	1596	20		0.59	3.79×10^{-11}
UT-4	1327	81[a]	12.5	1.4	4.30×10^{-12}[c]

---

[a] Oxidation done in air.

[b] Not measured.

[c] Calculated from total weight gain assuming parabolic kinetics throughout oxidation

[d] Not included in least squares analysis of temperature dependence of rate constants

Table II: Parabolic oxidation constants for powdered Si_3N_4 Calculated from the data of Tetard et al. for dry oxygen at 4 kPa (30 torr)

T, K	k_D° m^2/h	k_D, kg^2 m^{-4} s^{-1}
	Batch A (α/β = 2.0)	
1373	0.014	1.0×10^{-12}
1423	0.020	1.5×10^{-12}
1473	0.035	2.5×10^{-12}
1523	0.063	4.6×10^{-12}
1573	0.094	6.9×10^{-12}
	Batch B (α/β = 1.4)	
1373	0.004	3.2×10^{-13}
1423	0.006	4.1×10^{-13}
1473	0.010	7.5×10^{-13}
1523	0.013	9.7×10^{-13}
1573	0.038	2.8×10^{-12}

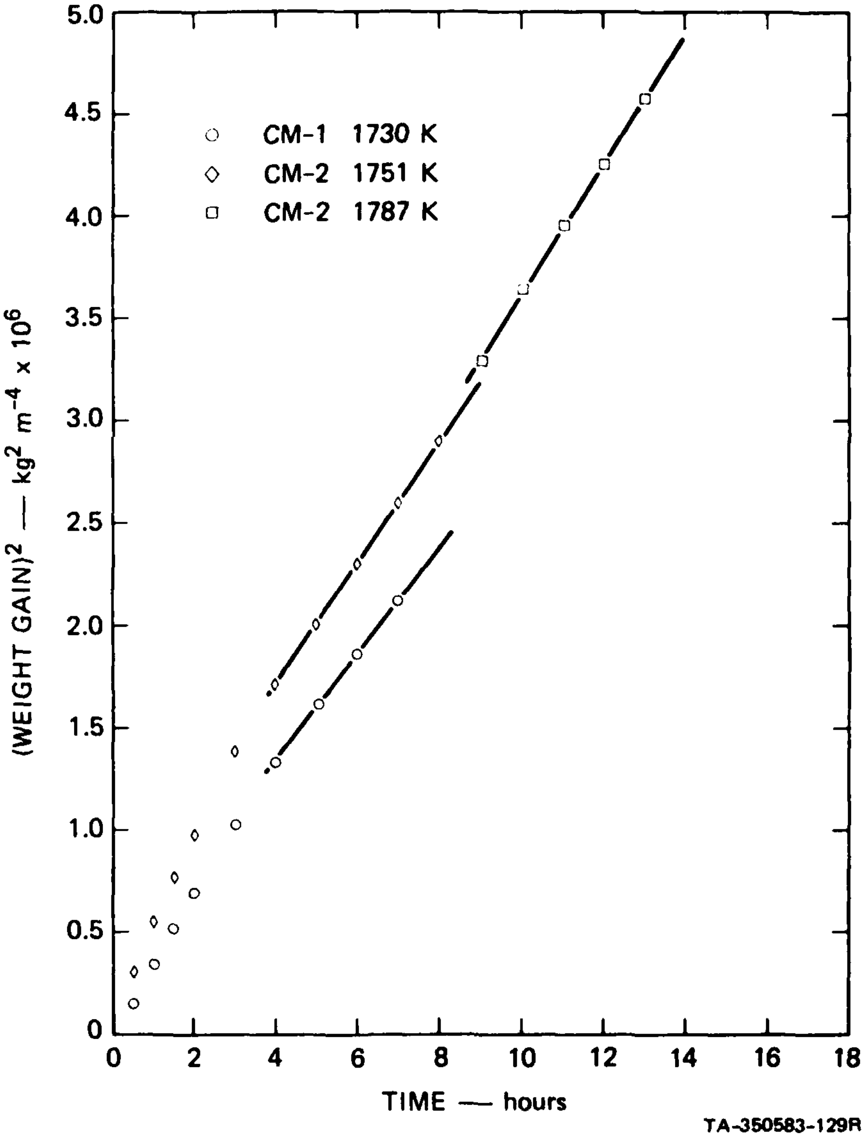

FIGURE 1 PARABOLIC PLOT OF THE OXIDATION OF CHEMETAL CVD SILICON NITRIDE SAMPLES

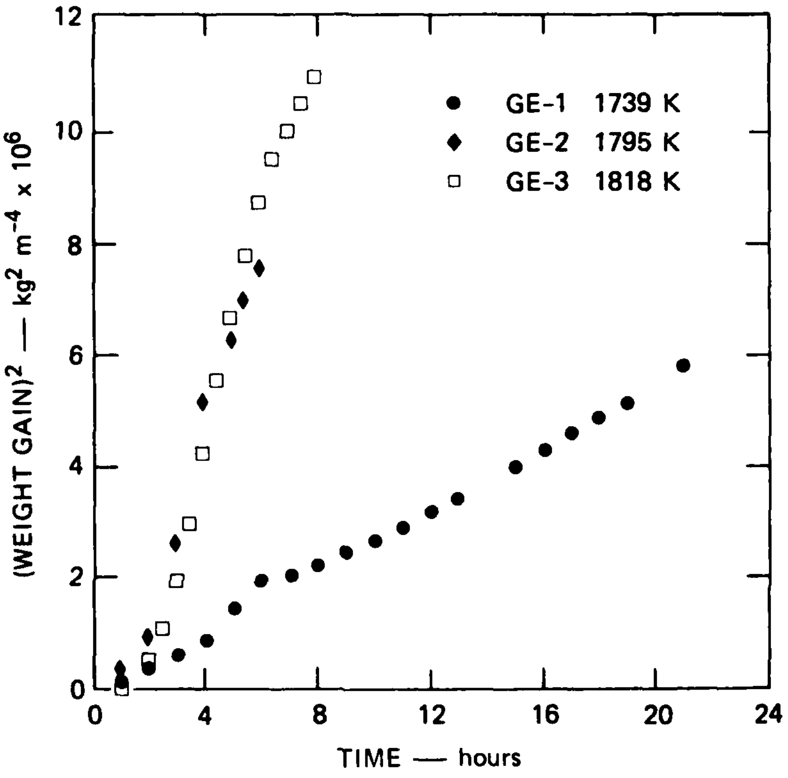

SA-5522-62R

FIGURE 2 PARABOLIC PLOT OF THE OXIDATION OF GENERAL ELECTRIC COMPANY CVD SILICON NITRIDE SAMPLES

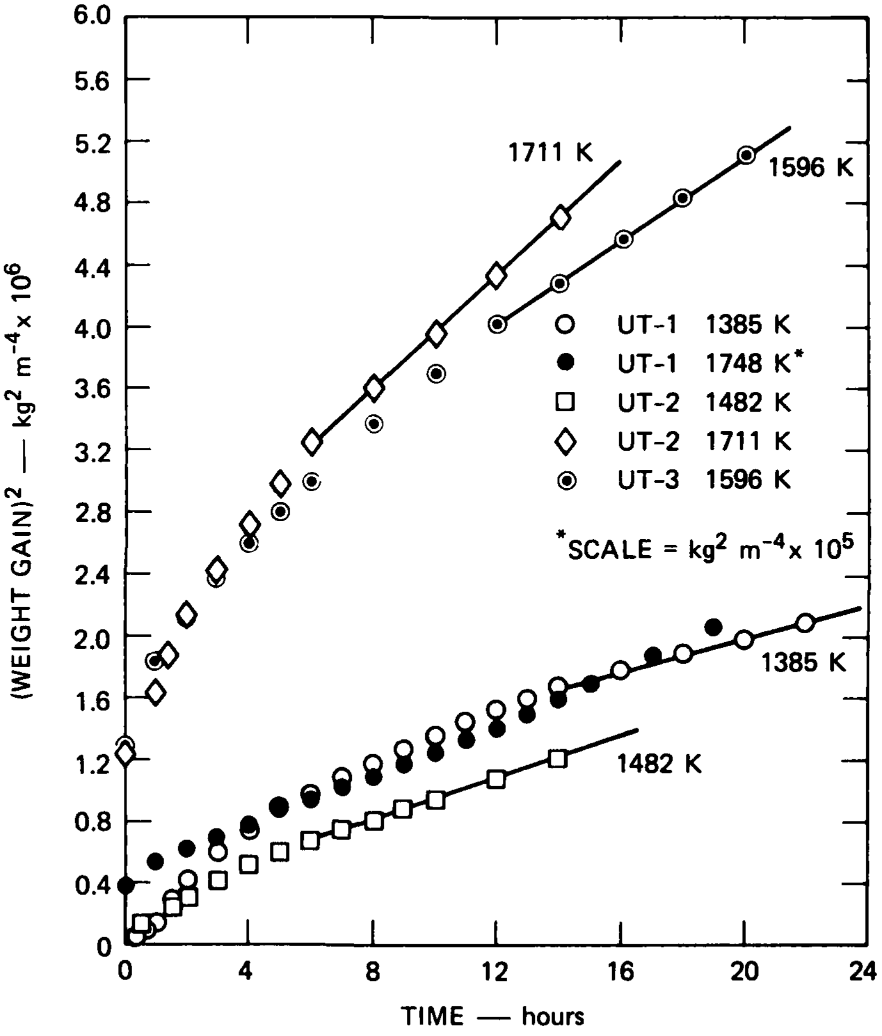

SA-5522-74

FIGURE 3 PARABOLIC PLOT OF THE OXIDATION OF UNITED TECHNOLOGIES CVD SILICON NITRIDE SAMPLES

SA-5522-75

FIGURE 4 UNOXIDIZED SPECIMEN OF UNITED TECHNOLOGIES CVD Si_3N_4. The rough deposition surface is at the top, above the fracture surface exhibiting columnar grain structure. (Width of Photograph = 0.2 mm.)

SA-5522-76

FIGURE 5 POLISHED CROSS SECTION OF UNOXIDIZED UNITED TECHNOLOGIES CVD Si_3N_4 EXHIBITING COLUMNAR GRAIN STRUCTURE WITH INTER-GRANULAR PORES. (Width of the Photograph = 0.5 mm.)

SA-5522-77

FIGURE 6 POLISHED CROSS SECTION OF OXIDE SCALE AND SUBSTRATE OF UNITED TECHNOLOGIES SAMPLE UT-1 OXIDIZED AT 1385 K FOR 22 HOURS AND AT 1748 K FOR 19 HOURS. (Width of the Photograph = 0.1 mm.)

SA-5522-78

FIGURE 7 SEM PHOTOGRAPH OF ADHERENT OXIDE SCALE AND SUBSTRATE OF UNITED TECHNOLOGIES SAMPLE UT-4 OXIDIZED 81 HOURS IN AIR AT 1325 K. (Width of the Photograph = 9×10^{-3} mm.)

TA-350583-130R

FIGURE 8 OXIDE SURFACE ON CHEMETAL SAMPLE CM-2 AFTER OXIDATION FOR 8 HOURS AT 1751 K AND 5 HOURS AT 1787 K. (Width of the Photograph = 0.1 mm.)

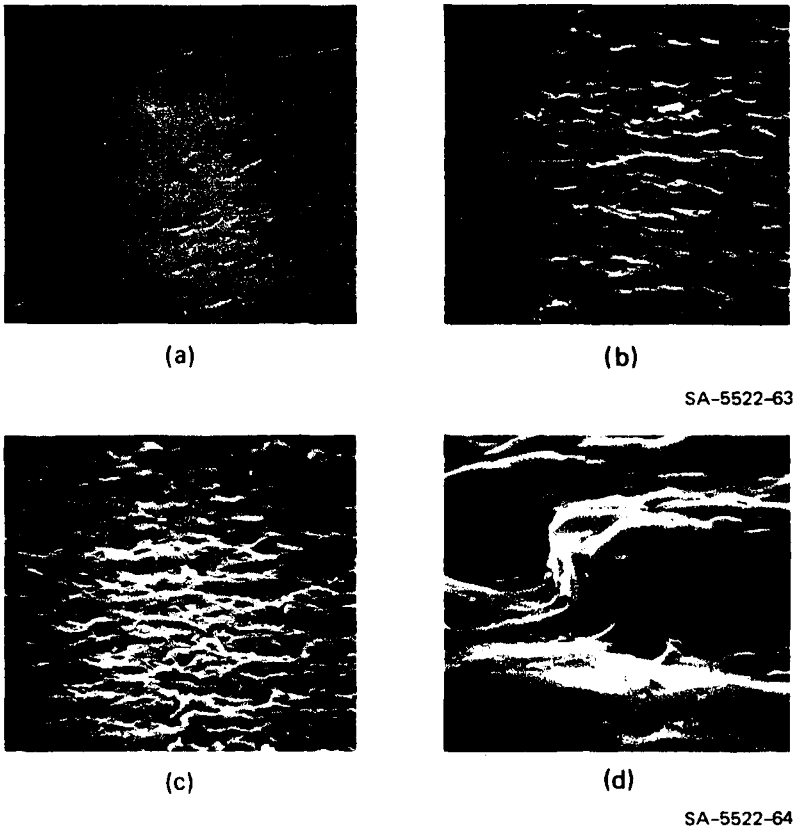

FIGURE 9 TAPER SECTION OF GENERAL ELECTRIC SAMPLE GE-3 OXIDIZED 8 HOURS AT 1818 K

a. Unattacked subsurface region on left, porous subscale region on right (Width of Photograph = 0.1 mm).

b. Taper-ground surface on left. The oxide layer on the unground surface flaked off during sectioning. (Width of photograph = 0.1 mm.)

c. Unground surface with part of oxide layer still attached. (Width of photograph = 0.1 mm.)

d. High magnification of unground surface with part of oxide layer still attached. (Width of photograph = 1 x 10^{-2}mm.)

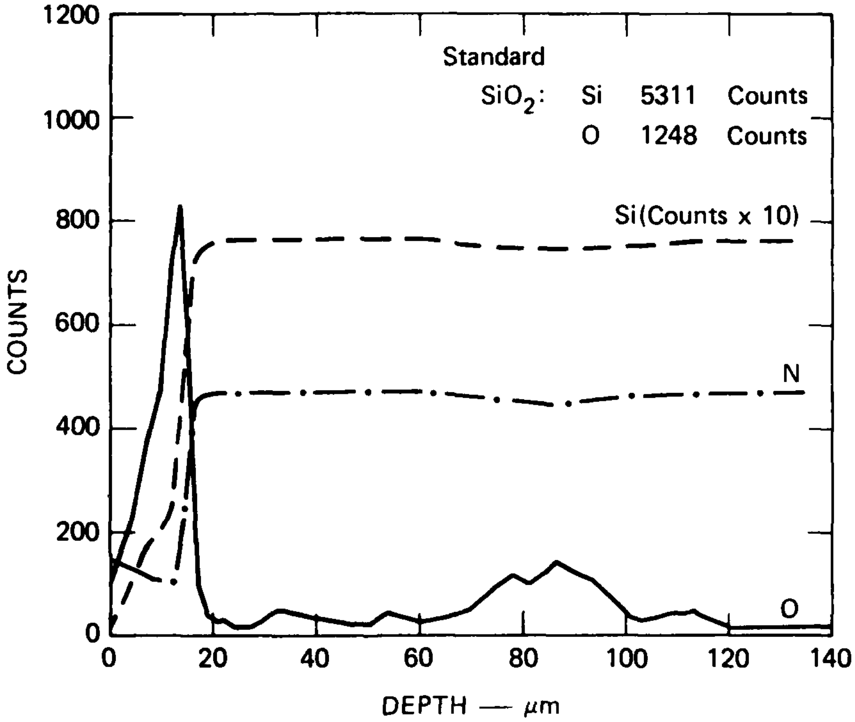

SA-5522-79

FIGURE 10 ELECTRON MICROPROBE SCANS OF Si, N, AND O THROUGH THE OXIDE SCALE OF SAMPLE UT-1 OXIDIZED 22 HOURS AT 1385 K AND 19 HOURS AT 1748 K.

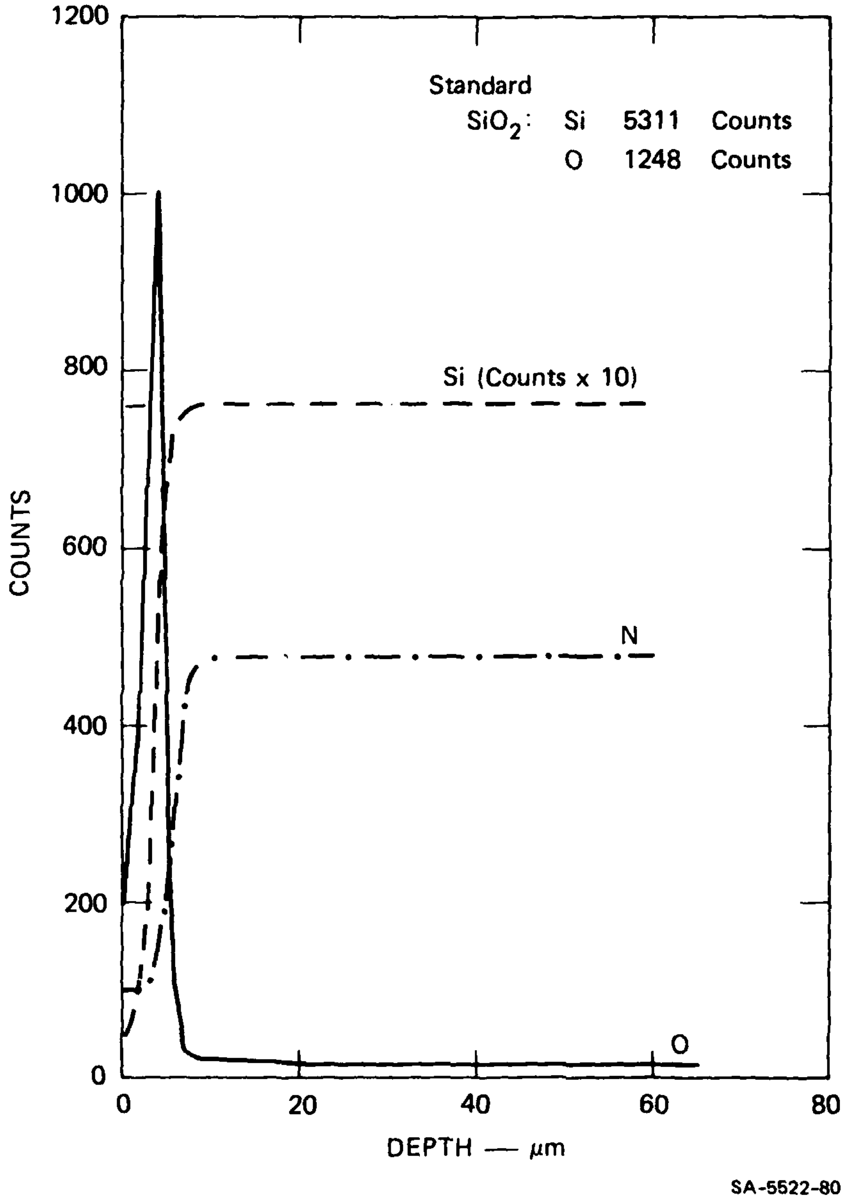

FIGURE 11 ELECTRON MICROPROBE SCANS OF Si, N, AND O THROUGH THE OXIDE SCALE OF SAMPLE UT-2 OXIDIZED 14 HOURS AT 1482 K AND 14 HOURS AT 1711 K.

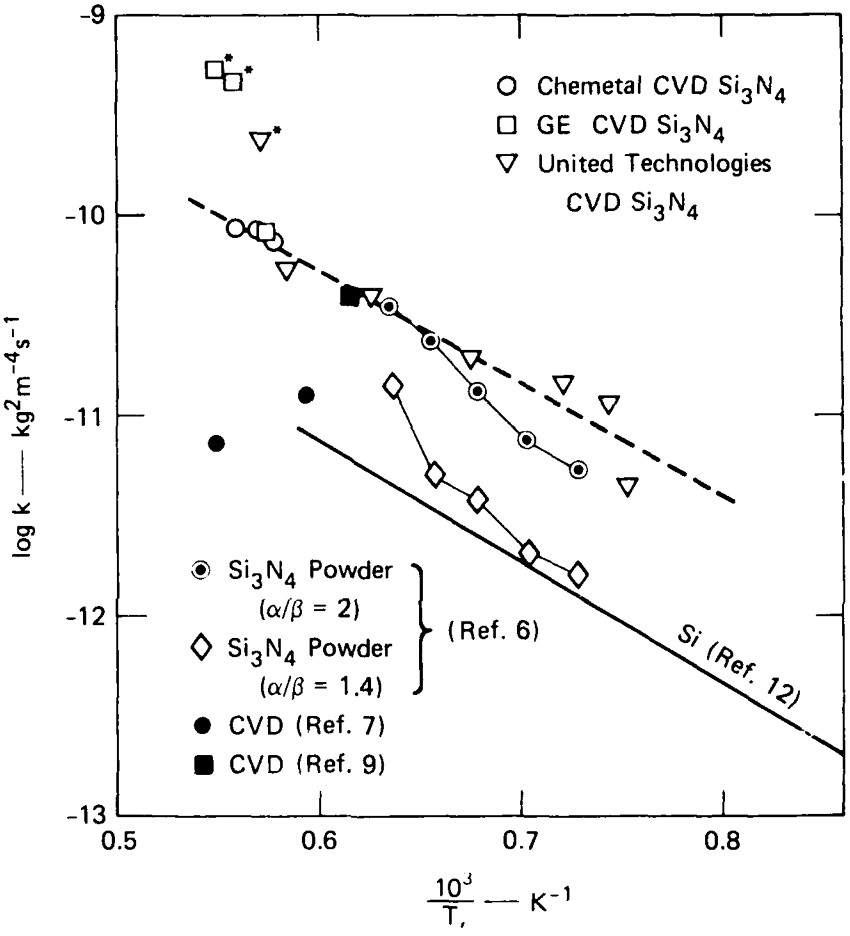

SA-5522-81

FIGURE 12 ARRHENIUS PLOT OF PARABOLIC OXIDATION CONSTANTS FOR SILICON,[11] POWDERED Si_3N_4,[6] AND CVD Si_3N_4.[7,9]

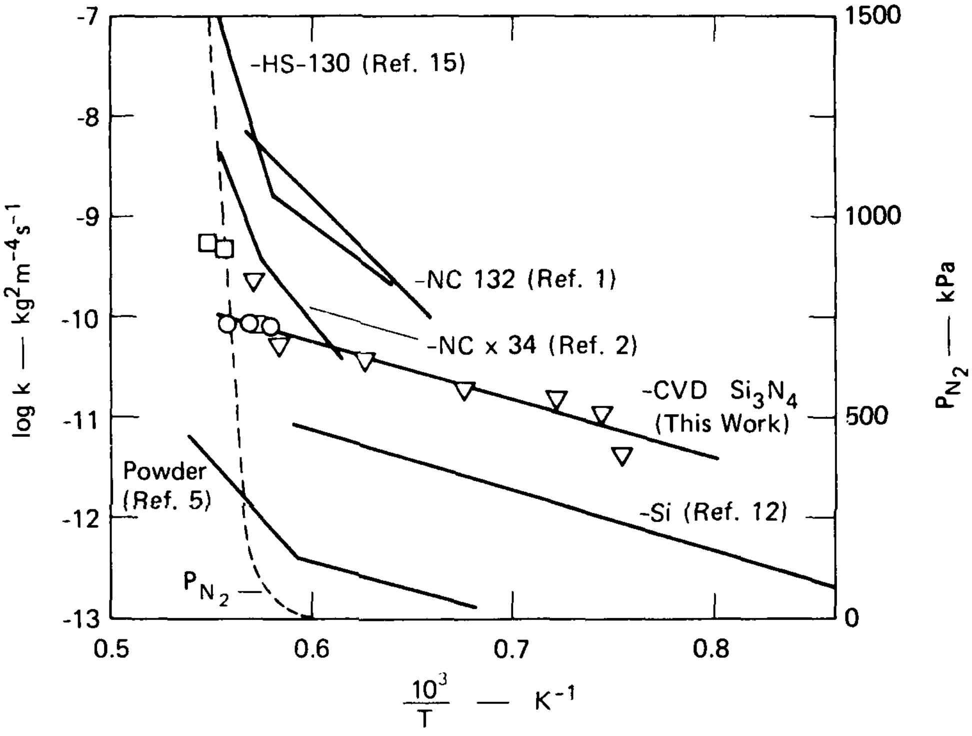

SA-5522-82

FIGURE 13 PARABOLIC OXIDATION CONSTANTS FOR HOT-PRESSED,[2,3] POWDERED,[5] AND CVD Si_3N_4, AND FOR SILICON.[12] The dashed line is the equilibrium nitrogen pressure for Reaction [3]. The oxidation constants for Si_3N_4 powder[5] were not corrected for the change in area during reaction.

DATE

ILMED

– 8